

2D excitation-emission fluorescence mapping analysis of plant food pigments

Raghavan Chinnamedu Murugesan, Mohammed Thofike Ahmed Choudhury, Alex Rozhin*

Nanoscience Research Group and The Wolfson Centre for Photonics for Food and Agri-Tech, Aston Institute of Photonic Technologies, College of Engineering and Physical Sciences, Aston University, Birmingham B4 7ET, United Kingdom

ARTICLE INFO

Keywords:

Pigment
Chlorophyll
Phenolic compounds
Carotenoids
Absorption
Fluorescence

ABSTRACT

Homogeneous dispersion of plant food pigments is indispensable to study their characteristic fluorescence features for non-destructive rapid monitoring of food systems. However, it is highly challenging to obtain such optical grade homogenized stable dispersion of various plant pigments in aqueous media for tracing their precise fluorescence signatures. Herein, we demonstrate a unique strategy to disperse various pigments, such as chlorophylls, carotenoids and phenolic compounds by the high-speed shear-force mixing of fresh green and red bell peppers (*Capsicum annuum*) in an aqueous medium with followed centrifugation and filtration. An advanced Fluorescence Excitation-emission (FLE) mapping and optical absorption analysis from the optical grade aqueous bell peppers dispersion allow simultaneous probing of chlorophylls, phenolic compounds and carotenoids by their characteristic electronic transitions. The demonstrated sampling protocols and spectroscopic analysis will be highly beneficial to obtain advanced spectroscopic databases from different food materials for rapid food analysis and quality control.

1. Introduction

The growing population of the Earth leads to many challenges associated with providing people access to energy sources, clean water and air, safe food. Based on the statistical data reported by the Food and Agriculture Organization of the United Nations, every year one-third of the globally manufactured food (about 1.3 billion tonnes) was wasted, costing roughly \$680 billion in industrialised countries and \$310 billion in developing countries (FAO, 2011). The food industry has an enormous number of safety and quality control challenges concerning microbiological and chemical contamination along the farm-to-fork food production chain. Traditionally, sampling for food analysis includes samples collection and preparation, enrichment, screening and confirmation of the pathogen. These stages involve knowledge-intensive processes such as extraction and separation, chromatography and analytical centrifugation, incubation and so on (Bae & Winemiller, 2018; Nielson, 2017; Ridgway et al., 2007; Verhoeckx et al., 2015). At the same time, the food industry is dependent on a large variety of analytical equipment for specific types of analysis such as chemistry analysis, food microbiology analysis, food nutrition analysis, allergens analysis, natural toxin analysis, food shelf-life study, nanomaterials

assisted analysis, etc (Corradini, 2018; Mustafa & Andreescu, 2020; Nielson, 2017; Sagoo et al., 2001; Wong & Lewis, 2017).

Among all analytical methods, Fluorescence (FL) spectroscopy offers a great advantage in food analysis through the use of FL labels or the direct detection of luminescent substances present in food systems, which include pigments, proteins, vitamins, secondary metabolites, toxins and flavouring compounds (Christensen et al., 2006; Sikorska & Khmelinskii, 2016; Sikorska, Khmelinskii, & Sikorski, 2012). Importantly, FL can use many parameters for sensing fluorophores such as changes in the intensity of FL bands and their spectral position, alterations in the intensity ratio of different bands and peaks, FL decay times, FL anisotropy, and variations in FL excitation wavelengths (Demchenko, 2015). Until recently, FL analysis was carried out mainly by bulk laboratory spectrometers giving highly sensitive results with good spectral resolution in different spectral ranges. However, the rapid development of electronics and microprocessor technology, observed over the past 10 years, made it possible to create miniature photoluminescence spectrometers integrated with laptops, tablets and smartphones (Das et al., 2016). Despite the limitations in the spectral resolution and sensitivity of the portable spectrometers, they can be effectively used for the express analysis of water and food samples. This can be achieved by

* Corresponding author.

E-mail address: a.rozhin@aston.ac.uk (A. Rozhin).

<https://doi.org/10.1016/j.foodchem.2023.135875>

Received 29 June 2022; Received in revised form 7 February 2023; Accepted 3 March 2023

Available online 6 March 2023

0308-8146/© 2023 The Authors. Published by Elsevier Ltd. This is an open access article under the CC BY license (<http://creativecommons.org/licenses/by/4.0/>).

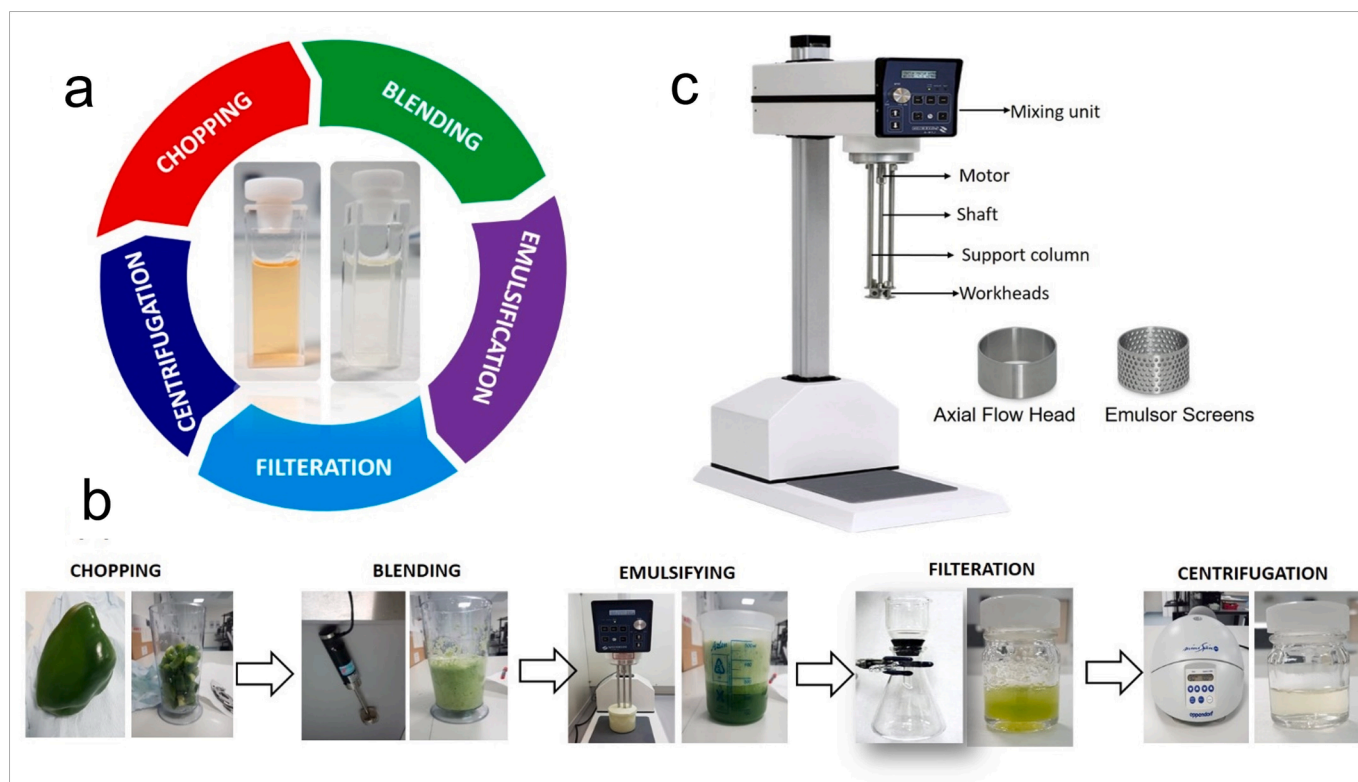


Fig. 1. Preparation of optical grade bell pepper aqueous solution a. Process flow for the preparation of green bell pepper (GBP) and red bell pepper (RBP) aqueous solution b. The Silverson L5M-A shear force mixer with axial flow work head and emulsor screens, which are used for the preparation of homogeneous optical quality bell pepper solution. c. Different stages in the extraction of GBP aqueous solution.

transferring express data via fiber optic and/or mobile networks to specialized servers containing high-precision laboratory FL data. Subsequent analysis using machine-learning methods will give an almost instant response on the content of harmful substances in the sample analysed by the mobile spectrometer.

While examining food samples, researchers typically explore the single wavelength excitation for FL spectra acquisition, which in turn required time-consuming sample preparation protocols with analytical chromatographic separation, chemical labelling, solid phase extraction and liquid-liquid extraction or other sample separation steps prior to the FL measurements (Sikorska & Khmelinskii, 2016; Sikorska, Khmelinskii, & Sikorski, 2012). Natural food samples contain a variety of complex chemical and biochemical (edible) fluorescence constituents, such as phenylalanine, tryptophan, vitamins, chlorophylls, etc (Christensen, 2005). Two-dimensional (2D) FL Excitation-emission (FLE) spectral mapping, which allows a set of FL emission spectra over the range of excitation wavelengths to be recorded, is highly feasible to analyse such complex food systems. The FLE spectroscopy is capable to detect at a time a whole class of pigments (for example carotenoids and chlorophylls) on one spectral map, because the spectral signatures of specific pigments will only appear in a certain range of excitation wavelengths.

Fluorescence spectroscopy with chemometric analysis has been used to classify a variety of foods, like dairy products, eggs, fish, meat, honey, and wine (Sádecká & Tóthová, 2007). Recently, the FLE mapping method was used for the validation of the quality of the dark brown sugars that were obtained through different processing conditions (Chen et al., 2021), and Rossi et al., 2021 used the FLE mapping method for the characterization of edible insect species. In this study, we have demonstrated a unique strategy for the optical grade dispersion of food pigments, namely chlorophylls, phenolic compounds, and carotenoids of fresh bell peppers (green and red) in aqueous media using shear force assisted mixing method (Paton, 2014) for Fluorescence detection without any chemical assistance. Their dispersion stability was

monitored for the 15 days aged samples using FLE spectral changes. We have chosen the bell pepper as an object of research, as an excellent phytonutrients source offering a range of carotenoids, which includes α -carotene, β -carotene, lutein, cryptoxanthin, zeaxanthin, etc, which have antioxidant and retina protection function for both animal and humans (Ekwere Mercy & Udo David, 2018; Feng et al., 2017). It is important to note, the conventional methods for the extraction and identification of carotenoids are mostly based on organic solvents (Alwis et al., 2015; Arvayo-Enríquez et al., 2013; Butnariu, 2016; Guiffreda et al., 2011; Lee et al., 2019). However, these methods rely on long extraction times and the consumption of a large volume of organic solvents during the extraction process, which in turn raises concerns about health and environmental hazards. Recently, Nagarajan et al. (2020) demonstrated a hydrocolloidal complexation strategy for the green extraction of carotenoids from Tomato Pomace in water media. The bell pepper aqueous solution obtained by the shear force assisted mixing method in this study allows for measuring distinct FL excitation-emission spectra for the phenolic compounds, carotenoids, and chlorophylls, simultaneously, from this analysis our study opens a new path for the green extraction of vegetable food pigments in water media.

2. Materials and methods

2.1. Extraction of optical grade bell pepper pigments

The 2D FLE spectroscopy relies on the homogeneous dispersion of fluorophores in a liquid medium to obtain a reliable excitation-emission mapping. To achieve such dispersion, we employed here a strategy of shear-force mixing of food material in an aqueous medium and successfully achieved extraction and the consequent dispersion of carotenoids, phenolic compounds and chlorophylls originated from the bell peppers (*Capsicum annuum*) as shown in Fig. 1. We preferred to use shear force mixing for the dispersion of various pigments of bell peppers,

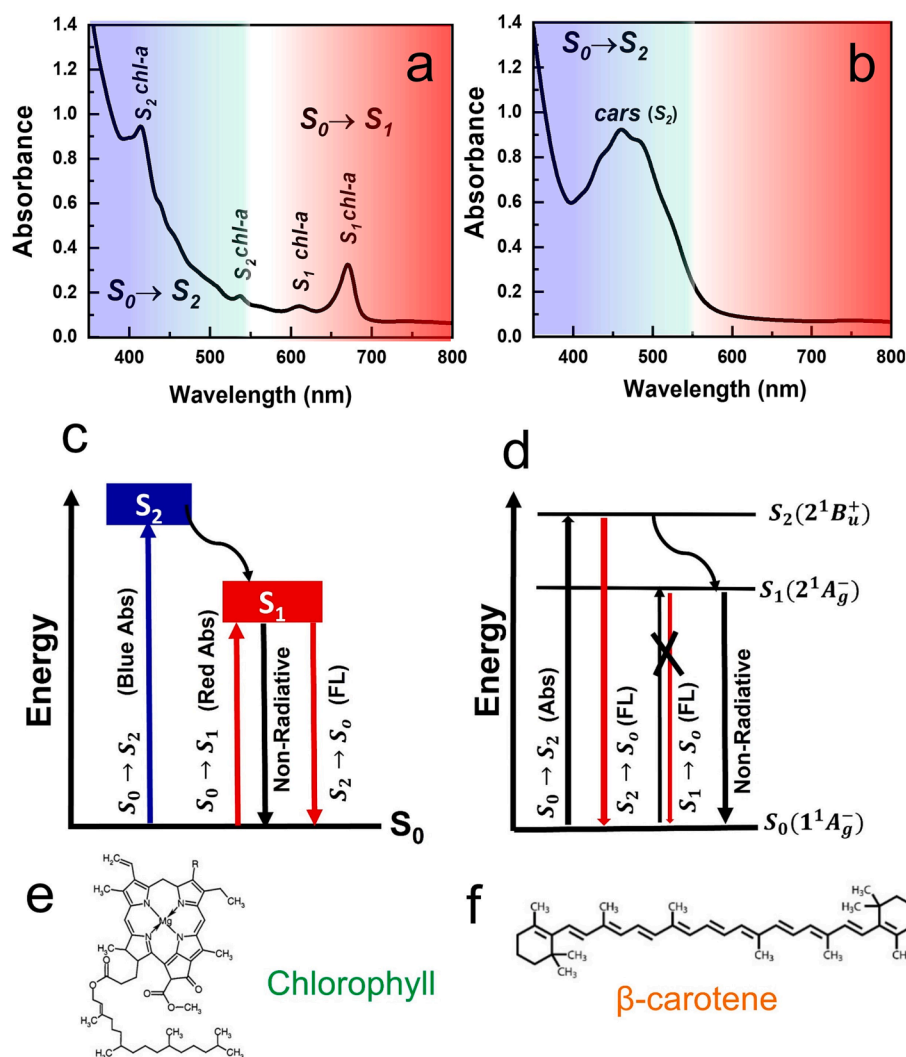


Fig. 2. Optical absorption spectra of a. GBP and b. RBP aqueous solution. c & d. The energy state diagram revealing electronic transition of *chl* and *car* constituents, respectively. The absorption bands in blue-green range (400–550 nm) corresponds to $S_0 \rightarrow S_2$ transition and the bands in red range (600–750 nm) corresponds to $S_0 \rightarrow S_1$ electronic transition of *chl-a* in GBP. The only *cars* absorption (400–600 nm) observed for RBP corresponding to $S_0 \rightarrow S_2$ transition of β -carotene. e & f. The chemical structures of chlorophyll and β -carotene, respectively.

because it offers efficient disintegration of aqueous insoluble organic solid species, especially carotenoids, into homogeneous distribution by generating high shear force (Paton, 2014) that can be achieved with specially designed axial flow and emulsor screen workheads and the complete procedure detailed in the *Extraction Method*.

2.1.1. Extraction method

The green bell pepper (GBP) and red bell pepper (RBP) were purchased from a local market and were used to prepare an advanced protocol for the optical quality solution in aqueous media. Fig. 1a illustrate the overall process involved in the preparation of an optical quality aqueous solution of bell peppers and Fig. 1b reveals various stages involved in the preparation of optical quality GBP solution. At first, the bell pepper (142 g) was chopped into small pieces using a kitchen knife. By using an immersive kitchen hand blender (Turbo, Ikich, operated at 400 W), the chopped bell pepper pieces blended into a slurry consisting of small solid pepper bits and the fluids released due to blending. To the resulting slurry, 300 ml of deionized water added as an aqueous dispersive media also helps to make the solution compatible with the high-speed shear force mixer. We have used the Silverson L5M-A shear force mixer configured with an axial flow head and an emulsor screen head (Fig. 1c), which has proven to be potential for generating high shear by closely spaced rotor/stator setup (Silverson Machine, 2022). At first, the mixer with the axial flow head was set at 3500 rpm for 60 min. While mixing, the high-speed rotation of the rotor blades connected with the precision-machined mixing workhead leads to

powerful suction and drawing liquid and solids pulps of pepper upwards from the bottom of the container into the centre of the workhead. Then, the materials are driven towards the periphery of the workhead by the centrifugal force where they undergo vigorous milling. An intense hydraulic shear due to high-speed rotors force materials out through the perforations in the stator and allows circulating into the main body of the mix. The process is continuous during the mixing period. The first choice of axial flow head was to expel aqueous pepper slurry vertically upwards to maintain heavy insoluble solids in liquid suspension for uniform distribution. In addition, it helps to disintegrate bigger solid pulp skins contained in the bell pepper solution.

Once these larger pieces disintegrated, the second settings with the emulsor screen were 5000 rpm and a 60 min duration with the same solution applied from the previous settings (the mixer head was cleaned before the second setting was applied). The high shear-force with the emulsor head attached was used to generate high turbulence for the homogenization of pigment fluorophores in the aqueous medium. For the green bell pepper, the aqueous solution obtained from the high-speed shear mixer was then subjected to vacuum assisted filtration using the Whatman glass microfiber filters having a pore size 0.7 μm . This is followed by centrifugation (MiniSpin, Eppendorf) at 10,000 rpm for 30 min to remove the fine solid pulps and membrane fibres through sedimentation. The resulting transparent solution is centrifuged again with the same previous settings to further separate any remaining substances. We used the same mixing protocol for the red bell pepper but the resulting solution required long centrifugation at 10,000 rpm for 1 hr

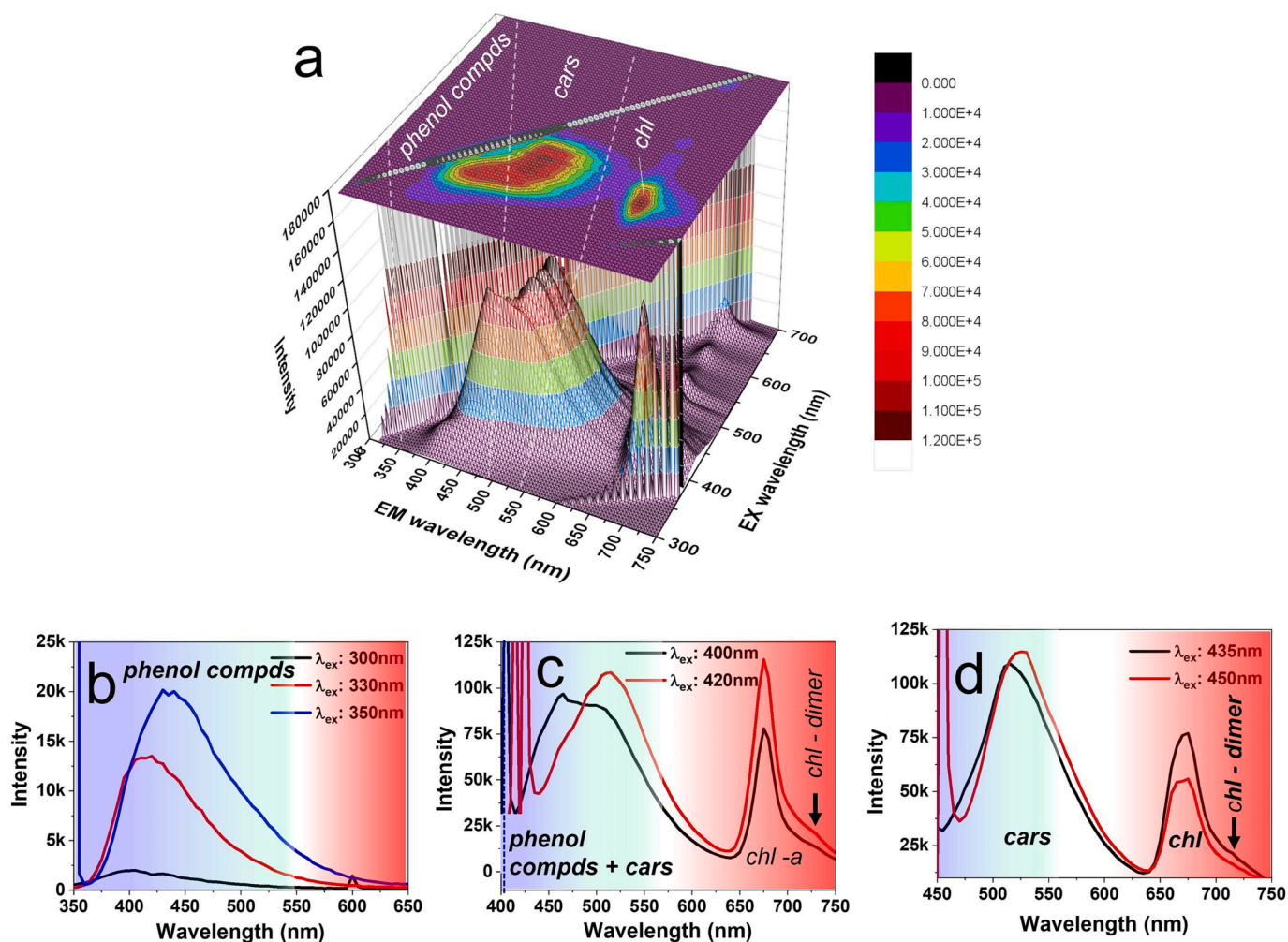


Fig. 3. a. Three-dimensional (3D) projection of FL spectrum obtained from the aqueous GBP solution. The top view of the projection shows FLE map with an intensity scale bars to reveal the dominant excitation-emission spots. Evolution of 3D FL emission spectra appeared inside the projection cage. The distribution of major pigments, such as *phenol compds*, *cars* and *chls* are indicated by the water lines on the FLE map. b. The FL spectra of *phenol compds* with dominated emission at $\lambda_{em} = 400\text{--}465\text{ nm}$ ($\lambda_{ex} = 300\text{--}350\text{ nm}$), c. *phenol compds* with evolution of *cars* appeared at $\lambda_{em} = 400\text{--}550\text{ nm}$ ($\lambda_{ex} = 400\text{--}420\text{ nm}$) and with predominant narrow *chl-a* emissions at $\lambda_{em} = 675\text{ nm}$ ($\lambda_{ex} = 420\text{ nm}$), and d. *cars* ($\lambda_{em} = 500\text{--}550\text{ nm}$) along with *chl-a* ($\lambda_{em} = 630\text{--}750\text{ nm}$) for the λ_{ex} : 435–450 nm.

30 min, due to excessive low density fibrous particulates floating in the solution. The Whatman glass microfiber filters 0.7 μm pores used to remove any micro membranes and other non-sediment low dense particulates suspended in the mixer. The pH value measured for the freshly prepared GBP aqueous solution was 6.7 and for the RBP aqueous solution 4.9, respectively. All the extraction procedure were conducted in the laboratory atmosphere at a temperature of 19 $^{\circ}\text{C}$ and humidity of 65 %, and the samples was stored at same conditions for 15 days to study the dispersion stability and changes in FLE spectral features.

2.2. Spectroscopic characterization

The optical absorption spectra of the aqueous bell pepper solution were measured with Lambda 1050 UV/VIS/NIR (Perkin Elmer) spectrometer featured with PMT, InGaAs and PbS three-detector module for the measurement of 170–3300 nm range. The FLE maps were recorded with Nanolog (Horiba Jobin Yvon) spectrofluorometer, equipped with a silicon (visible range) and InGaAs (NIR range) detectors, which allow measurement of excitation in the range from 270 to 800 nm and emission from 300 to 1600 nm. The InGaAs detector cooled with liquid nitrogen prior to measuring in the NIR spectral range. The entrance/exit slit width of 2 nm (for visible range) and 30 nm (NIR range) with an excitation interval 5 nm used for the monochromators. Chemical

constituents and elemental analysis for the dry solid products obtained from pepper solution were examined by X-ray photoelectron spectroscopy (XPS). The XPS measurement is limited to solid samples. Therefore, to make the dry solids of GBP and RBP, 10 ml of aqueous bell pepper solution obtained through a shear force-assisted mixing method was poured onto the Petri dish and allowed slow evaporation at a constant temperature of 50 $^{\circ}\text{C}$ for 24 h in a hotplate. Thus, the obtained well-dry solids of GBP and RBP were used for the XPS measurements using ThermoFisher ESCALAB 250 electron spectrometer equipped with a hemispherical sector energy analyser. A monochromatic Al K α X-ray source was used for analysis to enhance the resolution. XPS measurements were carried out at source excitation energy of 15 KeV and emission current of 6 mA; analyser pass energy of 50 eV with a step size of 0.1 eV and dwell time of 50 ms.

3. Results and discussion

3.1. Optical absorption and electronic transition analysis

Different colours of fruits and vegetables are primarily occurred due to dominant pigment groups, such as chlorophylls (green), carotenoids (yellow-orange-red), phenolic compounds and anthocyanin (red-blue-purple), and betanin (red) (Rodriguez-Amaya, 2016). To reveal

characteristic absorption and emission features of the bell pepper pigments in aqueous media, the optical absorption spectra (Fig. 2a and 2b) are split into two blue-green (between 400 and 550 nm) and red (between 600 and 750 nm) spectral ranges. Typically, carotenoids (*cars*) exhibit characteristic absorption in the blue-green range and chlorophyll (*chl*) absorbs in both blue-green and red spectral ranges (Jhonson, 2016).

From Fig. 2a, the GBP aqueous solution shows sharp absorption peaks at wavelengths of 415 nm, 537 nm, 613 nm, and 670 nm, respectively. The formation of the majority of these absorption bands are well correlated to the electronic transition of the delocalized π -electrons of the *chl* species (Jhonson, 2016; Milenković et al., 2012). Based on the energy state diagram (Fig. 2c), *chl* has two excited states, (S_1) and (S_2) and the ground state (S_0). The energy gap between the ground state (S_0) and the first excited state (S_1) spans the wavelengths ranging from 600 nm to 750 nm and the energy gap between (S_0) and the second excited state (S_2) spans around 400 nm and 550 nm. As shown in Fig. 2a, a sharp absorption peak at 415 nm and a small spectral spike at 537 nm are ascribed to $S_0 \rightarrow S_2$ electronic transition and the sharp absorption at 670 nm and a weak band at 613 nm are due to $S_0 \rightarrow S_1$ transition of the chlorophyll-a (*chl-a*) molecule. All spectral features of Fig. 2a are in good agreement with the electronic transitions (Fig. 2c) of a monomer of *chl-a* molecule (Brown, 1969; Croce et al., 2000; Frias et al., 2018; Milenković et al., 2012). The chemical structure of *chl* is represented by the combination of porphyrin head having a central magnesium ion (Mg^{2+}) and a long hydrocarbon tail (Fig. 2e). The R-group attached to the porphyrin classifies a different class of *chl* molecules, such as *chl-a* ($R = CH_3$), *chl-b* ($R = CHO$) and etc. The porphyrin head with conjugated π -electrons is primarily responsible for the above spectroscopic properties (Jhonson, 2016; Milenković et al., 2012). Moreover, the formation of the absorption band at 613 nm (Fig. 2a) reveals the aggregation of *chl-a* molecules in aqueous media (Frias et al., 2018). There are very weak absorption bands between 450 and 550 nm (Fig. 2a), can be related to the contribution of both *chl* and *cars* (Croce et al., 2000; Frias et al., 2018).

From Fig. 2b, the RBP aqueous solution shows absorption features only in the range between 400 and 550 nm, which are well correlated with carotenoids. There is no absorption related to chlorophylls indicating the complete absence of chlorophylls in the RBP aqueous solution. Carotenoids are derivatives of polyenes, in which conjugated π -bonds are responsible for the unique spectroscopic features (Jhonson, 2016; Lichtenthaler, 1987). The absorption spectrum shown in Fig. 2b reveals two absorption maxima at 464 and 486 nm and one shoulder peak at 436 nm. The observed spectral shape and peak position of this absorption spectrum is closely correlated to the characteristic spectral features of β -carotene (Fig. 2f) (Alwis et al., 2015; Lichtenthaler, 1987; Rivera Vélez, 2016). Fig. 2d shows the energy state diagram of carotenoids, in which the ground state $S_0(1^1A_g^-)$ and two excited states, such $S_1(2^1A_g^-)$ and $S_2(1^1B_u^+)$ are involved in the electronic transition (Bondarev, 1997; Lichtenthaler, 1987). The term symbols ($1^1A_g^-$) and ($2^1B_u^+$) are representing the symmetry of the orbital energy state that are typically used to describe the allowed and forbidden electronic transition of carotenoids (Bondarev, 1997; Feng et al., 2017). The spectroscopically allowed $S_0 \rightarrow S_2(1^1A_g^- \rightarrow 1^1B_u^+)$ electronic transition is the origin of absorption of *cars* in the blue-green range (400–550 nm), while the transition between the ground state to the first excited state $S_0 \rightarrow S_1(1^1A_g^- \rightarrow 2^1A_g^-)$ is forbidden transition (Fig. 2d) (Bondarev, 1997).

3.2. FL excitation emission features of aqueous bell pepper pigments

FL spectroscopy offers great advantages over optical absorption spectroscopy because it can be detected against a low background, making use of this spectroscopy with high sensitivity, capable to detect extremely low concentrations of food pigments even down to parts per billion (Sikorska & Khmelinskii, 2016). As food systems contain a

collection of various pigments, the resulting FL spectra will also have a multi-peak spectral feature with emission contribution from different pigments. A fine selection of the wavelength of the FL excitation will make it possible to dominate the emission of a specific pigment, which will lead to a redistribution of the FL emission maxima. Therefore, the FL Excitation emission (FLE) mapping of food samples is highly beneficial in the rapid detection and assigning of food fluorophores for fingerprint identification. However, it highly relies on the optically transparent homogeneous solution that can be able to provide bright and clear resonant emissions.

3.2.1. Green bell pepper FLE mapping analysis

Fig. 3a shows the three-dimensional (3D) projection of FL Excitation emission (FLE) mapping obtained from the GBP aqueous solution. The measurement was carried out in the excitation wavelengths ranging from 300 nm to 700 nm with an excitation increment 5 nm and the emission wavelengths ranging from 300 nm to 750 nm. The top view of the 3D projection is plotted by 2D FLE contour mapping with intensity scale bars to reveal the dominant excitation- emission spots with different emission centres covered by two distinct spectral ranges in the blue-green (λ_{em} : 400 nm–550 nm) and red regions (λ_{em} : 600 nm–750 nm). Evolution of 3D FL spectra with different sets of FL emission for different groups of pigments dispersed in aqueous GBP in the overall range of excitation appears inside the projection cage. The major group of FL components present in GBP aqueous solution, such as phenolic compounds (*phenol compds*) with FL in the range 450–500 nm ($\lambda_{ex} = 300$ –400 nm), *cars* with FL 500–550 nm ($\lambda_{ex} = 400$ –450 nm) and *chl* with FL in the range 650–750 nm ($\lambda_{ex} = 400$ –420 nm) are represented by the water lines at Fig. 3a. The FL spectra extracted for the dominant excitation emission wavelengths are shown in Fig. 3b–3d, respectively. Fig. 3b shows the FL emission peaks at λ_{em} 440 nm ($\lambda_{ex} = 350$ nm), 415 nm ($\lambda_{ex} = 330$ nm) and 400 nm ($\lambda_{ex} = 300$ nm) respectively, which are typically reveal the presence of different *phenol compds* (Giampaoli et al., 2020). From Fig. 3b–3c, FL emission shows increasing trends of intensity in the λ_{ex} between 300 nm and 420 nm. The formation of intense broad FL emission peak λ_{em} 400–450 nm for the λ_{ex} 300–350 nm can be closely correlated with the group of hydroxycinnamic acids (ferulic acid, coumaric acid, and caffeic acid), which comes under the family of phenolic compounds (Lichtenthaler & Schweiger, 1998; Meyer et al., 2003). From Fig. 3c, the observed intense emission peak at the λ_{em} of 675 nm ($\lambda_{ex} = 400$ –450 nm) is in good agreement with the $S_1 \rightarrow S_0$ electronic transition of the monomer *chl-a* species (Frias et al., 2018; Jhonson, 2016) as shown in Fig. 2c. The maximum intensity of FL for *chl-a* is observed at the λ_{ex} of 420 nm (Fig. 3c). The formation of a weak shoulder peak at 720 nm associated with the sharp FL emission peak of *chl-a* (Fig. 3c and 3d) reveals its dimerization (Brody & Brody, 1962; Frias et al., 2018). The emissions at the λ_{em} of 515 nm ($\lambda_{ex} = 420$ –435 nm) and 525 nm ($\lambda_{ex} = 450$ nm) (Fig. 3c and 3d) are well correlated with the FL emission of *cars* species and in particular with $S_2 \rightarrow S_0(1^1B_u^+ \rightarrow 1^1A_g^-)$ electronic transition (Fig. 2d) (Kandori et al., 1994; Kleinegris et al., 2010). At the λ_{ex} of 400 nm, the broad emission with multiple emission maxima of λ_{em} of 465 nm and 505 nm (Fig. 3c) indicated the contribution of both *phenol compds* and *cars* in the FL spectrum (Fatchurrahman et al., 2015; Kleinegris et al., 2010; Lichtenthaler & Schweiger, 1998).

In overall consideration, the FL emission observed in the blue-green spectral range for GBP aqueous solution can be correlated to the collective FL emission of carotenoids ($\lambda_{em} = 505$ –550 nm) (Cherry et al., 1968; Kandori et al., 1994; Kleinegris et al., 2010) and phenolic compounds ($\lambda_{em} = 400$ –465 nm) (Giampaoli et al., 2020; Lichtenthaler & Schweiger, 1998). The FL emission in the red range ($\lambda_{em} = 600$ –750 nm) for the different excitation confirms the presence of chlorophylls and pheophytin in the GBP aqueous solution (Diaz et al., 2003; Frias et al., 2018; Jhonson, 2016; Milenković et al., 2012). The clear distinct bright emission spots in FLE mapping and the evolution of intense luminescence in the projection cage clearly reveal the high optical quality of the aqueous

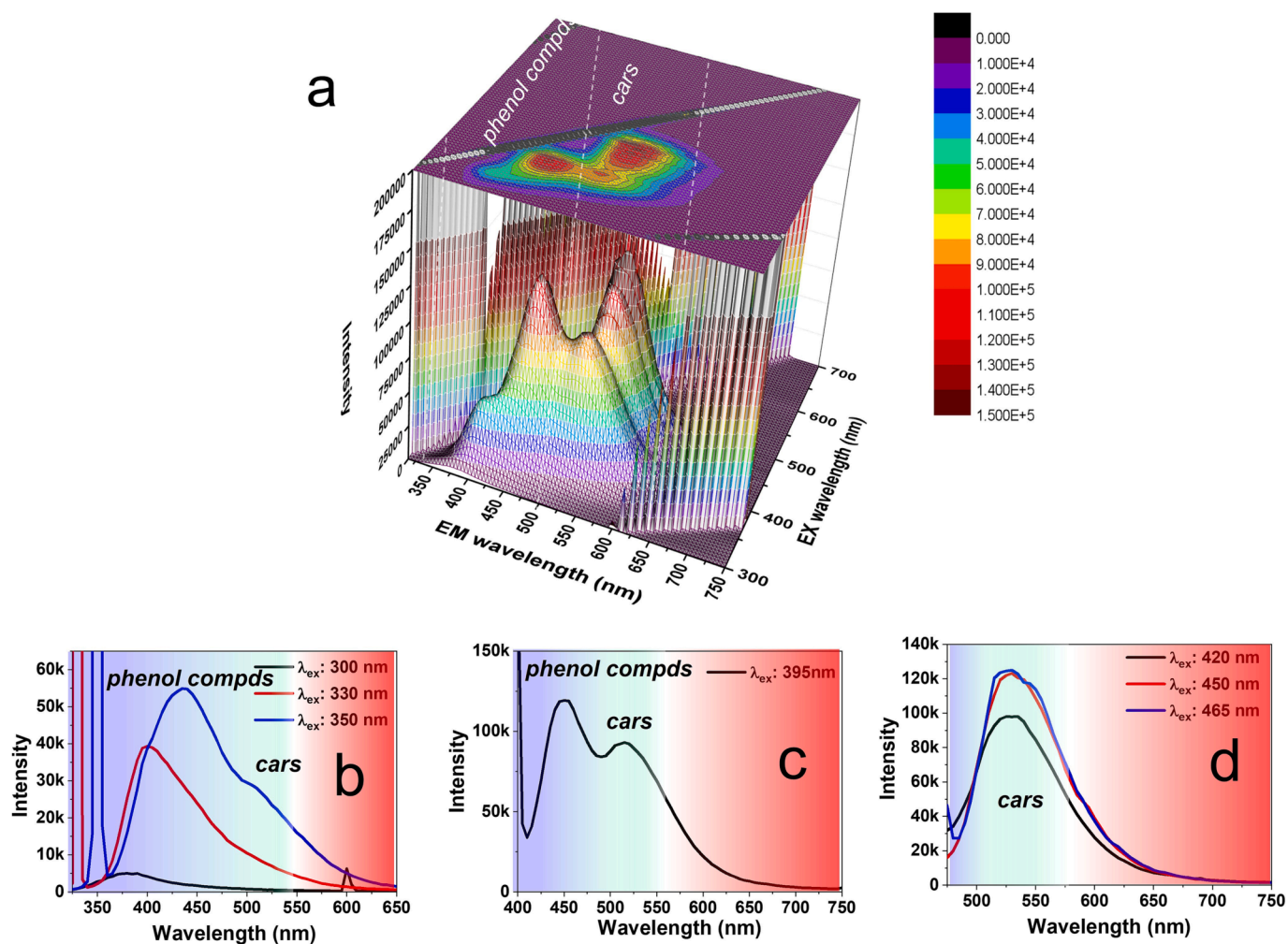


Fig. 4. a. The 3D projection of FL spectroscopic results obtained from the RBP aqueous solution. The FLE contour map top view with an intensity scale bars to reveal the excitation and emission features of different pigments. The RBP shows dominant emission only in blue-green spectral range ($\lambda_{em} = 350\text{ nm}–550\text{ nm}$) for *phenol compds* and *cars* with the complete absence of *chl* emission. The extracted FL spectra of: b. *phenol compds* with mild *cars* emission appeared at λ_{em} between 400 nm and 550 nm ($\lambda_{ex} = 300–350\text{ nm}$); c. *phenol compds* at the $\lambda_{em} = 448\text{ nm}$ and *cars* at the $\lambda_{em} = 515\text{ nm}$ ($\lambda_{ex} = 395\text{ nm}$); d. *cars* emission with λ_{em} between 500 nm–550 nm ($\lambda_{ex} = 400–465\text{ nm}$).

GBP solution obtained by the shear-force mixing process.

3.2.2. Red bell pepper FLE mapping analysis

The 3D projection of FL spectroscopic results obtained from the optical quality RBP aqueous solution is shown in Fig. 4a. The RBP shows dominant emission only in the blue-green spectral range (350–550 nm) with the complete absence of *chl* emission. Fig. 4b shows the FL spectra with the emission maxima λ_{em} shifted from 385 to 435 nm, when excitation wavelength λ_{ex} increases from 300 to 350 nm. All these peaks are correlated to the phenolic compounds (Giampaoli et al., 2020; Lichtenthaler & Schweiger, 1998; Meyer et al., 2003). Additionally, these spectra show an increase in the FL intensity by ~ 11 times with an increase in the excitation wavelength from 300 to 350 nm (Fig. 4b). The FL spectrum obtained with excitation of 350 nm shows the appearance of a spectral shoulder at about 515 nm (Fig. 4b), which indicates the contribution of *cars* (Kandori et al., 1994). A further increase in the excitation wavelength to 395 nm (Fig. 4c) leads to the registration of two peak spectra with maxima at about 448 and 515 nm, which are typically associated with ferulic acid and carotenoids (Kandori et al., 1994; Lichtenthaler & Schweiger, 1998; Wang et al., 2017), respectively. Besides, the FOODFLOUR library also associated PL in the range of 515 nm with the presence of vitamin B2 (Christensen, 2005). Fig. 4d demonstrates intense broadband PL with a maximum at about 530 nm upon

excitation λ_{ex} at 420–465 nm. What is very important, the spectra have features in the region of 550 and 600 nm (Fig. 4d), which indicates the influence of different carotenoids such as neoxanthin (Mimuro et al., 1992) and vitamin B2 on the integral spectrum.

There are distinct bright FL emission spots (Fig. 4a) in the range between 500 and 550 nm for the FL excitations between 400 nm and 450 nm, which clearly indicates the existence of different carotenoids in RBP aqueous solution. The bright FL emission obtained in the range between 500 and 550 nm (Fig. 4a) is in good agreement with the $S_2 \rightarrow S_0(1^1B_u^+ \rightarrow 1^1A_g^-)$ electronic transition for carotenoids (Fig. 2d) (Bondarev, 1997; Lichtenthaler, 1987). The formation of $\lambda_{em} 530\text{ nm}$ is due to the electronic transitions in low-lying singlet S_2 electronic states of the β -carotene (Kandori et al., 1994). Based on the literature reports, there is a strong relationship between FL emission wavelengths and the molecular structure of carotenoids (Mimuro et al., 1992). In our study, the FL emission for both GBP and RBP aqueous solution is occurred between 500 nm and 550 nm, which due to $S_2(1^1B_u^+) \rightarrow S_0(1^1A_g^-)$ transition of carotenoids. The overall FL emission spectra obtained at different sets of excitation ranges between 300 nm and 500 nm, which are given in Supporting Information (S1) for the GBP (Fig. S1a and S1b) and the RBP (Figs. S1c and S1d), reveal the emission of phenolic compounds, carotenoids and chlorophyll for GBP and phenolic compounds and

Table 1

Elemental analysis of red and green pepper aqueous solution evaporated at 50 °C.

Red Bell Pepper		Green Bell Pepper	
Elements	Relative Atomic (%)	Elements	Relative Atomic (%)
C—C/C—H	51.7	C—C/C—H	37.1
C—O	18.6	C—O	23.9
C=O	2.2	C=O	4.3
O—C=O	3.1	O—C=O	2.4
C—N	1.8	C—N	1.9
O1s	19.7	O1s	27.8
N	1.8	N	1.8
K	0.4	K	0.4
P	0.2	P	0.2
Si	0.2	F	0.1
F	0.2	S	0.1
S	0.2	Mg ²⁺	< 0.1

carotenoids for RBP respectively.

3.3. XPS and FTIR analysis-Microenvironment of aqueous bell pepper pigments

Apart from pigments, there are other components, such as sugars

(saccharides and carbohydrates), vitamins, organic species and minerals are present in bell peppers. During shear mixing, the soluble components of the above ingredients could act as a microenvironment in the extracted optical quality solution. In order to observe these components, we have further extended the characterization with X-ray photoelectron spectroscopy (XPS) and Fourier transform infrared (FT-IR) spectral analysis. For these analyses, the aqueous pepper solution was dried by evaporation at 50 °C. The well-dried evaporation products of GBP and RBP solids were used for the FT-IR and XPS analysis. The FT-IR spectra of GBP and RBP are shown in [Supporting Information \(Figs. S2a and S2b\)](#). There is no significant difference in the FT-IR spectrum of the GBP and RBP solid products that were obtained by the evaporation of optical quality pepper solution. Most of the functional groups associated with the FTIR bands in both GBP and RBP originated from dissolved sugars (carbohydrates, saccharides), phenolic compounds, amino acids, aromatic phosphates and epoxy components. All FTIR bands of GBP and RBP with their corresponding functional groups are listed in the [Supporting Information Table 1 \(SI-Table 1\)](#). In addition, the presence of various organic functional groups/elements (micro-nutrients) with their relative atomic percentage obtained through XPS analysis from GBP and RBP samples are given in [Table 1](#). Most of the organic functional groups obtained in the FT-IR well correlate with the XPS results. Consequently, the dissolved sugars, alkaloids and minerals are the microenvironments

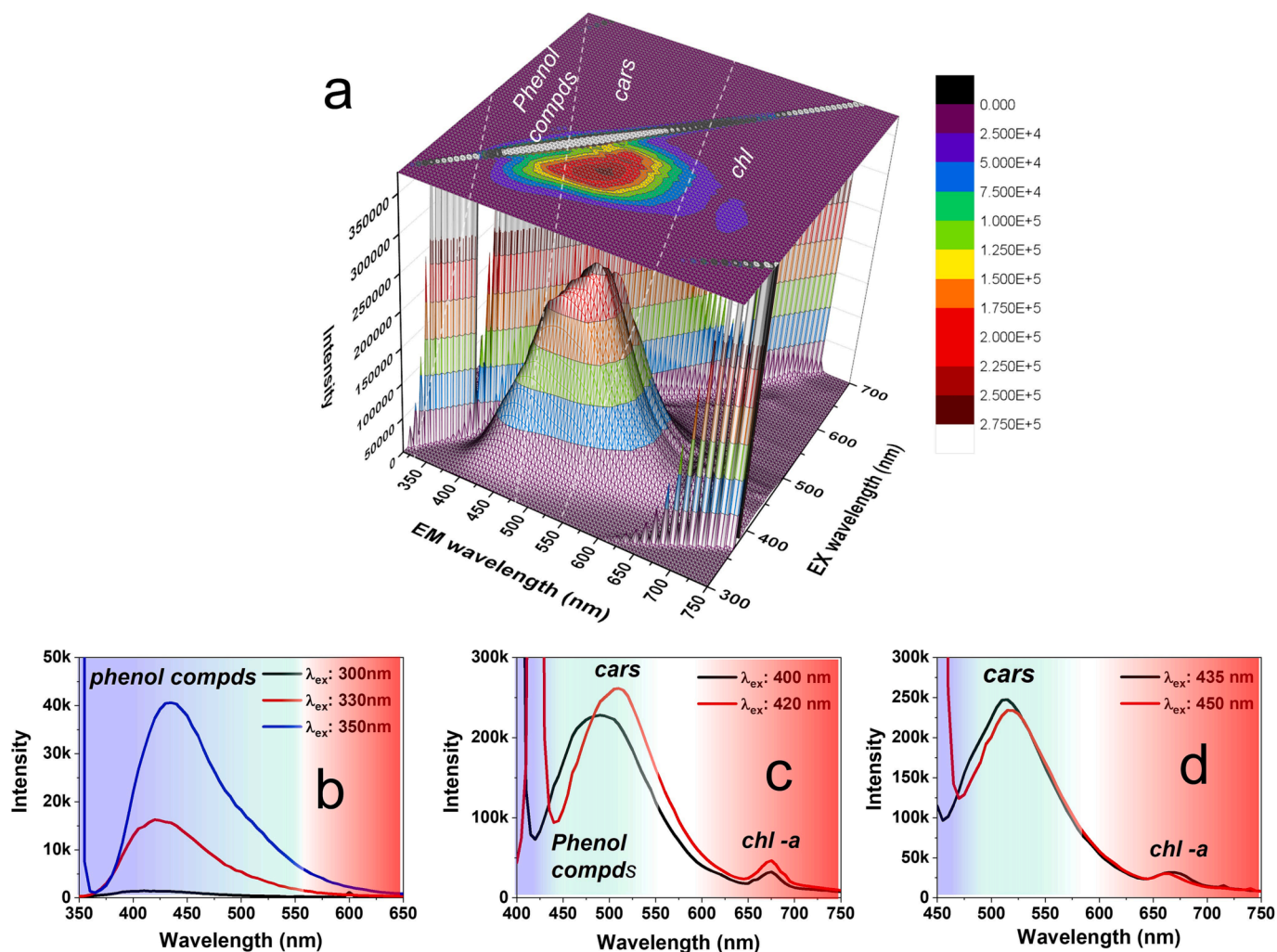


Fig. 5. a. 3D projection of FL spectroscopic results obtained from the 15 days aged GBP aqueous solution. The FL emission related to *phenol compds* and *cars* in the blue-green range, the λ_{em} between 350 and 550 nm are dominated, while, the *chl-a* emission in red range, the λ_{em} between 600 nm and 750 nm, got significantly quenched. The FL spectra extracted for the dominant excitation-emissions of: b. *phenol compds* (λ_{em} = 400–500 nm for the λ_{ex} = 300–350 nm); c & d *cars* (λ_{em} = 500–550 nm for the λ_{ex} = 400–450 nm) and *chl* (λ_{em} = 600–750 nm for the λ_{ex} = 400–450 nm), respectively.

for dispersed pigment fluorophores in the aqueous medium. Moreover, the absence of Mg^{2+} ion in red bell pepper clearly reveals the absence of chlorophyll, which is well consistent with the FLE mapping.

3.4. FL stability of the aqueous bell pepper pigments

To monitor the stability of the optical quality aqueous GBP and RBP solution, we have examined changes in fluorescence features of the 15 days aged samples. Fig. 5a shows a 3D projection of FL spectroscopic mapping results obtained from the 15 days aged GBP aqueous solution and the results demonstrated at the same excitation conditions of fresh GBP aqueous solution. As shown in Fig. 5a, the FL resonant spot associated with *chl-a* constituent of the GBP aqueous solution is significantly quenched. The blue-green spectral fluorophores (phenolic and carotenoid compounds) dominate FL emissions (Fig. 5b–5d). The FL intensity of *chl-a* observed at λ_{em} of 675 nm (λ_{ex} = 420 nm) for 15 days aged GBP solution decreased more than twice (Fig. 5c) when compared to the fresh sample (Fig. 3c). At the same time, the FL emission intensity of both the *phenol compd* (λ_{ex} = 350 nm, Fig. 5b) and *cars* (λ_{ex} = 435–450 nm, Fig. 5d) increases about two times for aged GBP solution compared to fresh GBP solution (Fig. 3b and 3d). The *cars* broad FL band was observed at 490 nm (λ_{ex} = 400 nm, Fig. 5c) for the aged GBP solution, while the fresh GBP solution, at the same excitation condition, shows FL with two emission bands associated with *phenol compd* (λ_{em} = 465 nm) and *cars* (λ_{em} = 505 nm) respectively (Fig. 3c). Furthermore, the FL intensities at 490 nm (λ_{ex} = 400 nm) and 515 nm (λ_{ex} = 420 nm) for the aged GBP (Fig. 5c) are increased two times as compared to the freshly prepared GBP aqueous solution. There are no de-metallized pheophytin (*chl* without Mg^{2+}) emission spots in the aged sample, which are observed in the fresh GBP solution. From this study, the 15 days aged GBP aqueous solution showed a significant decrease in the FL emission intensity of chlorophylls, which indicates the chemical degradation of chlorophyll components, whereas, the FL emission intensity at blue-green region corresponding to the phenolic compounds and carotenoids increased. The increase in FL intensity in the blue-green region of the aged GBP solution might be attributed to the formation of oxidative by-products of phenolic compounds and carotenoids and resonance energy transfer in the surrounding chemical environment. In contrast, the aged samples of RBP aqueous solution showed decreased FL intensity at the blue-green spectral region when compared to the fresh sample, indicating the different chemical environment in the RBP solution. The changes in fluorescence features of the 15 days aged RBP aqueous solution with results and discussion are shown in Supporting Information (S3, Figs. S3a–d).

4. Conclusions

In summary, we showed that the shear force-assisted mixing process following centrifugation and filtration offers an advanced sampling protocol for optical quality bell pepper aqueous solution achieved without the aid of any chemical assistance. The high optical quality of GBP and RBP solutions plays a vital role in fine fluorescence sensing of chlorophylls, phenolic compounds and carotenoids simultaneously in the complex environments through the 2D FLE spectroscopic analysis. The proposed sampling technique and the rapid spectroscopic detection can be extended to other food systems such as vegetables, fruits, meat and pulses. As demonstrated in the present work, the development of a food pigments data library, obtained through 2D FLE mapping for various fluorophores of the different food materials, would be highly beneficial in the sensing and rapid monitoring of food quality applications, which in turn tremendously help to control global food waste.

CRedit authorship contribution statement

Raghavan Chinnambedu Murugesan: Conceptualization, Methodology, Investigation, Data curation, Analysis, Validation, Writing –

original draft, Writing – review & editing. **Mohammed Thofike Ahmed Choudhury:** Methodology, Investigation, Data Curation, Formal Analysis. **Alex Rozhin:** Conceptualization, Supervision, Investigation, Validation, Writing – review & editing, Resources, Funding acquisition.

Declaration of Competing Interest

The authors declare that they have no known competing financial interests or personal relationships that could have appeared to influence the work reported in this paper.

Data availability

Data will be made available on request.

Acknowledgements

The authors (Raghavan Chinnambedu Murugesan and Alex Rozhin) acknowledge the support of the Marie Skłodowska-Curie Individual Fellowship (MOFUS, # 795356) and of the Wolfson Foundation. Raghavan Chinnambedu Murugesan, Mohammed Thofike Ahmed Choudhury, and Alex Rozhin acknowledge the support of the Enabling Technologies & Innovation Competences Challenge (ETICC) Project, partly funded by the European Regional Development Funds (ERDF). The authors would like to acknowledge Prof John Sullivan and Dr Baogui Shi from Midlands Surface Analysis Ltd for the insightful suggestion and valuable discussion on XPS measurement and analysis. Authors would like to thanks to Dr Khalid Doudin, FTIR and NMR specialist, of Chemical Engineering and Applied Chemistry Department, Aston University for the FTIR spectral analysis and discussion.

Data availability

Data will be made available via Aston University's Research Data Repository and on request.

Appendix A. Supplementary data

Supplementary data to this article can be found online at <https://doi.org/10.1016/j.foodchem.2023.135875>.

References

- Alwis, H. D. D. D., Chandrika, U. G., & Jayaweera, P. M. (2015). Spectroscopic studies of natural and chemically oxidized species of β -carotene, lycopene and norixin in CH_2Cl_2 : Fluorescence from intermediate compounds. *Journal of Luminescence*, 158, 60–64. <https://doi.org/10.1016/j.jlumin.2014.08.036>
- Arvayo-Enríquez, H., Mondaca-Fernández, I., Gortáez-Moroyoqui, P., López-Cervantes, J., & Rodríguez-Ramírez, R. (2013). Carotenoids extraction and quantification: Review. *Analytical Methods*, 5(12), 2916–2924. <https://doi.org/10.1039/C3AY26295B>
- Bae, S. Y., & Winemiller, M. D. (2018). Trace level analysis of sarin and VX in food using normal phase silica gel and ultra-performance liquid chromatography–time-of-flight mass spectrometry (UPLC–TOF–MS). *Journal of Agricultural and Food Chemistry*, 66(29), 7846–7856. <https://doi.org/10.1021/acs.jafc.8b01756>
- Bondarev, S. L. (1997). Photophysics of β -carotene and compounds. *Journal of Applied Spectroscopy*, 64, 1–15. <https://doi.org/10.1007/BF02683481>
- Brody, S. S., & Brody, M. (1962). Fluorescence properties of aggregated chlorophyll in vivo and in vitro. *Transactions of the Faraday Society*, 58, 416–428. <https://doi.org/10.1039/TF9625800416>
- Brown, J. S. (1969). Absorption and fluorescence of Chlorophyll a in particle fractions from different plants. *Biophysical Journal*, 9(12), 1542–1552. [https://doi.org/10.1016/S0006-3495\(69\)86469-6](https://doi.org/10.1016/S0006-3495(69)86469-6)
- Butnariu, M. (2016). Methods of analysis (extraction, separation, identification and quantification) of carotenoids from natural products. *Journal of Ecosystem & Ecography*, 6(2), 1000193. <https://doi.org/10.4172/2157-7625.1000193>
- Chen, J.-Y., Chen, X.-W., Lin, Y.-Y., Yen, G.-C., & Lin, J. A. (2021). Authentication of dark brown sugars from different processing using three-dimensional fluorescence spectroscopy. *LWT*, 150, Article 111959. <https://doi.org/10.1016/j.lwt.2021.111959>
- Cherry, R. J., Chapman, D., & Langelaar, J. (1968). Fluorescence and Phosphorescence of β -Carotene. *Transactions of the Faraday Society*, 64, 2304–2307. <https://doi.org/10.1039/TF9686402304>

- Christensen, J. (2005). FOODFLUOR- Food Fluorescence Library, <http://www.models.kvl.dk/foodfluor>.
- Christensen, J., Nørgaard, L., Bro, R., & Engelsen, S. B. (2006). Multivariate autofluorescence of intact food systems. *Chemical Reviews*, 106(6), 1979–1994. <https://doi.org/10.1021/cr050019q>
- Corradini, M. G. (2018). Shelf life of food products: From open labeling to real-time measurements, *Annual Review of Food Science and Technology*, 9, 251–269. <https://doi.org/10.1146/annurev-food-030117-012433>.
- Croce, R., Cinque, G., Holzwarth, A. R., & Bassi, R. (2000). The Soret absorption properties of carotenoids and chlorophylls in antenna complexes of higher plants. *Photosynthesis Research*, 64, 221–231. <https://doi.org/10.1023/A:1006455230379>
- Das, A. J., Wahi, A., Kothari, L., & Raskar, R. (2016). Ultra-portable, wireless smartphone spectrometer for rapid, non-destructive testing of fruit ripeness. *Scientific Reports*, 6, 32504. <https://doi.org/10.1038/srep32504>
- Demchenko, A. P. (2015). *Introduction to fluorescence sensing*. Springer Nature. <https://doi.org/10.1007/978-3-319-20780-3>.
- Diaz, T. G., Mera, I. D., Correa, C. A., Roldan, B., & Caceres, M. I. R. (2003). Simultaneous fluorometric determination of chlorophylls a and b and pheophytins a and b in olive oil by partial least-squares calibration. *Journal of Agricultural and Food Chemistry*, 51(24), 6934–6940. <https://doi.org/10.1021/jf034456m>
- Ekwere Mercy, R., & Udo David, E. (2018). Potential health benefits of conventional nutrients and phytochemicals of Capsicum peppers. *Pharmacy & Pharmacology International Journal*, 6(1), 62–69. 10.15406/ppij.2018.06.00157.
- FAO. 2011. Gustavsson, J., Cederberg, C., Sonesson, U., van Otterdijk, R., & Rome, A. M. Global food losses and food waste: extent, causes and prevention, www.fao.org/docrep/014/mb060e/mb060e00.pdf.
- Fatchurrahman, D., Kuramoto, M., Ogawa, Y., Kondo, N., & Suzuki, T. (2015). Identification of UV-fluorescence components associated with and detection of surface damage in green pepper (*Capsicum annuum* L.). In WSCG 2015 Conference on Computer Graphics, Visualization and Computer Vision. ISBN 978-80-86943-65-7.
- Feng, J., Tseng, C.-W., Chen, T., Leng, X., Yin, H., Cheng, Y.-C., et al. (2017). A new energy transfer channel from carotenoids to chlorophylls in purple bacteria. *Nature Communication*, 8, 71. <https://doi.org/10.1038/s41467-017-00120-7>
- Frias, A. R., Pecoraro, E., Correia, S. F. H., Minas, L. M. G., Bastos, A. R., García-Revilla, S., et al. (2018). Sustainable luminescent solar concentrators based on organic–inorganic hybrids modified with chlorophyll. *Journal of Materials Chemistry A*, 6(18), 8712–8723. <https://doi.org/10.1039/C8TA01712C>
- Giampaoli, P., Fernandes, F. F., Tavares, A. R., Domingos, M., & Cardoso-Gustavson, P. (2020). Fluorescence emission spectra of target chloroplast metabolites (flavonoids, carotenoids, lipofuscins, pheophytins) as biomarkers of air pollutants and seasonal tropical climate. *Environmental Science and Pollution Research*, 27, 25363–25373. <https://doi.org/10.1007/s11356-020-08646-y>
- Guiffrida, D., Dugo, P., Dugo, G., Torre, G., & Mondello, L. (2011). Analysis of native Carotenoid composition of sweet bell peppers by serially coupled C30 Columns. *Natural Product Communications*, 6, 1817–1820. <https://doi.org/10.1177/1934578X1100601207>
- Jhonson, M. P. (2016). Photosynthesis. *Essays in Biochemistry*, 60(3), 255–273. <https://doi.org/10.1042/EBC20160016>
- Kandori, H., Sasabe, H., & Mimuro, M. (1994). Direct determination of a lifetime of the S₂ state of β-Carotene by femtosecond time-resolved fluorescence spectroscopy. *Journal of American Chemical Society*, 116(6), 2671–2672. <https://doi.org/10.1021/ja00085a078>
- Kleinegris, D. M. M., van Es, M., Janssen, M. A., Brandenburg, W. A., & Wijffels, R. H. (2010). Carotenoid fluorescence in *Dunaliella salina*. *Journal of Applied Phycology*, 22, 645–649. <https://doi.org/10.1007/s10811-010-9505-y>
- Lee, J., Song, J., Lee, D., & Pang, Y. (2019). Metal-enhanced fluorescence and excited state dynamics of carotenoids in thin polymer films. *Scientific Reports*, 9, 3551. <https://doi.org/10.1038/s41598-019-40446-4>
- Lichtenthaler, H. K. (1987). Chlorophylls and carotenoids: Pigments of photosynthetic biomembranes. *Methods in Enzymology*, 148, 350–382. [https://doi.org/10.1016/0076-6879\(87\)48036-1](https://doi.org/10.1016/0076-6879(87)48036-1)
- Lichtenthaler, H. K., & Schweiger, J. (1998). Cell wall bound ferulic acid, the major substance of the blue-green fluorescence emission of plants. *Journal of Plant Physiology*, 152(2–3), 272–282. [https://doi.org/10.1016/S0176-1617\(98\)80142-9](https://doi.org/10.1016/S0176-1617(98)80142-9)
- Meyer, S., Cartelat, A., Moya, I., & Cerovic, Z. G. (2003). UV-induced blue-green and far-red fluorescence along wheat leaves: A potential signature of leaf ageing. *Journal of Experimental Botany*, 54(383), 757–769. <https://doi.org/10.1093/jxb/erg063>
- Milenković, S. M., Zvezdanović, J. B., Anđelković, T. D., & Marković, D. Z. (2012). The identification of chlorophyll and its derivatives in the pigment mixtures: HPLC chromatography, visible and mass spectroscopy studies. *Advanced Technologies*, 1(1), 16–24.
- Mimuro, M., Nagashima, U., Takaichi, S., Nishimura, Y., Yamazaki, I., & Katoh, T. (1992). Molecular structure and optical properties of carotenoids for the in vivo energy transfer function in the algal photosynthetic pigment system. *Biochimica et Biophysica Acta (BBA) – Bioenergetics*, 1098(2), 271–274. [https://doi.org/10.1016/S0005-2728\(05\)80347-0](https://doi.org/10.1016/S0005-2728(05)80347-0)
- Mustafa, F., & Andreescu, S. (2020). Nanotechnology-based approaches for food sensing and packaging applications. *RSC Advances*, 10, 19309–19336. <https://doi.org/10.1039/D0RA01084G>
- Nagarajan, J., Kay, H.P., Krishnamurthy, N.P., Ramakrishnan, N.R., Aldawoud, T.M. S., Galanakis, C. M., & Wei O.C. (2020). Extraction of carotenoids from tomato pomace via water-induced hydrocolloidal complexation. *Biomolecules*. 10(7): 1019. doi: 10.3390/biom10071019.
- Nielson, S. S. (2017). *Food analysis* (5th ed.). Springer Nature. Doi: 10.1007/978-3-319-45776-5.
- Paton, K. R., et al. (2014). Scalable production of large quantities of defect-free few-layer graphene by shear exfoliation in liquids. *Nature Materials*, 13, 624–630. <https://doi.org/10.1038/nmat3944>
- Ridgway, K., Lalljie, P. D., & Smith, R. M. (2007). Sample preparation techniques for the determination of trace residues and contaminants in foods. *Journal of Chromatography A*, 1153(1–2), 36–53. <https://doi.org/10.1016/j.chroma.2007.01.134>
- Rivera Vélez, S. M. (2016). Guide for carotenoid identification in biological samples. *Journal of Natural Products*, 79(5), 1473–1484. <https://doi.org/10.1021/acs.jnatprod.5b00756>
- Rodriguez-Amaya, D. B. (2016). Natural food pigments and colorants. *Current Opinion in Food Science*, 7, 20–26. <https://doi.org/10.1016/j.cofs.2015.08.004>
- Rossi, G., Durek, J., Ojha, S., & Schlüter, O. K. (2021). Fluorescence-based characterisation of selected edible insect species: Excitation emission matrix (EEM) and parallel factor (PARAFAC) analysis. *Current Research in Food Science*, 4, 862–872. <https://doi.org/10.1016/j.crf.2021.11.004>
- Sádecká, J., & Tóthová, J. (2007). Fluorescence spectroscopy and chemometrics in the food classification – a review. *Czech Journal of Food Sciences*, 25(4), 159–173. <https://doi.org/10.17221/687-CJFS>
- Sagoo, S. K., Little, C. L., & Mitchell, R. T. (2001). The microbiological examination of ready-to-eat organic vegetables from retail establishments in the United Kingdom. *Letters in Applied Microbiology*, 33(6), 434–439. <https://doi.org/10.1046/j.1472-765X.2001.01026.x>
- Sikorska, E., Khmelinskii, I., & Sikorski, M. (2012). Analysis of olive oils by fluorescence spectroscopy: methods and applications. In Olive oil - Constituents, quality, health properties and bioconversions, Boskou, D. (Ed.) *InTech*, 4, 63–88. DOI: 10.5772/30676.
- Sikorska, E., & Khmelinskii, I. (2016). Glowing colours of foods: Application of fluorescence and chemometrics in food studies. *Spectroscopy Europe*, 28(6), 10–13. <https://www.spectroscopyeurope.com/article/glowing-colours-foods-application-fluorescence-and-chemometrics-food-studies>.
- Silverson Machine-High Speed High Shear Mixers-Laboratory Mixers <https://www.silverson.co.uk/>. (last update April 10th, 2020).
- Verhoeckx, K. C. M., Vissers, Y. M., Baumert, J. L., Faludi, R., Feys, M., Flanagan, S., et al. (2015). Food processing and allergenicity. *Food and Chemical Toxicology*, 80, 223–240. <https://doi.org/10.1016/j.fct.2015.03.005>
- Wang, S., Schatz, S., Stuhldreier, M. C., Böhnke, H., Wiese, J., Schröder, C., et al. (2017). Ultrafast dynamics of UV-excited trans- and cis-ferulic acid in aqueous solutions. *Physical Chemistry Chemical Physics*, 19(45), 30683–30694. <https://doi.org/10.1039/C7CP05301K>
- Wong Y., & Lewis, R. J. (2017). Analysis of food toxins and toxicants, *Wiley Blackwell Volumes 1 & 2*.